Am J Transl Res 2025;17(7):4894-4911
www.ajtr.org /ISSN:1943-8141/AJTR0163474

Original Article

Study of NOX4/ROS/NF-κB signaling pathway in anti-ischemia-reperfusion injury effect and mechanism of STQJD

Caiying Luo[1*], Li Zhang[1*], Aiyun Wang[1], Yuting Wang[1], Jing Cai[1], Ruoyan Ni[1], Renhua Yang[1,3], Sijin He[2], Lihua Gu[2], Peng Chen[1,3]

[1]School of Pharmaceutical Sciences and Yunnan Key Laboratory of Pharmacology for Natural Products, Kunming Medical University, Kunming 650500, Yunnan, China; [2]Department of Rehabilitation, Kunming Municipal Hospital of Traditional Chinese Medicine, Kunming 650599, Yunnan, China; [3]College of Modern Biomedical Industry, Kunming Medical University, Kunming 650500, Yunnan, China. [*]Equal contributors and co-first authors.

Received January 21, 2025; Accepted June 12, 2025; Epub July 15, 2025; Published July 30, 2025

Abstract: Objective: This study aimed to investigate the effects of Shu-Tiao Qi-Ji Decoction (STQJD) on a rat model of cerebral ischemia-reperfusion injury and to elucidate its mechanism of action. Methods: The therapeutic effects of STQJD on ischemic stroke (IS) were assessed using neurobehavioral scores, 2,3,5-Triphenyltetrazolium chloride (TTC), Nissl and Terminal deoxynucleotidyl transferase dUTP nick end labeling (TUNEL) staining. Network pharmacology was used to investigate the potential mechanisms of STQJD. Reactive Oxygen Species (ROS) content and expression levels of inflammatory markers in rat serum were detected. The mRNA and protein expression levels of Nuclear factor kappa-light-chain-enhancer of activated B cells (NF-κB), NADPH oxidase 4 (NOX4), Tumor necrosis factor-alpha (TNF-α), NOD-like receptor family pyrin domain containing 3 (NLRP3), Apoptosis-associated speck-like protein containing a CARD (ASC), Toll-like receptor 4 (TLR4), and Cysteine-dependent aspartate-specific protease-1 (Caspase-1) in the brain tissue of rats were detected using RT-qPCR and Western blotting. Immunofluorescence was used to detect NF-κB and TNF-α protein expression. Results: STQJD markedly improved neurological function, reduced cerebral infarct volume, and mitigated neuronal damage and apoptosis in rats subjected to Middle Cerebral Artery Occlusion (MCAO). Gene Ontology (GO) and Kyoto Encyclopedia of Genes and Genomes (KEGG) analyses revealed that STQJD's anti-IS effects are linked to NOX4/TLR4/NF-κB/TNF-α signaling pathways. STQJD reduced serum levels of inflammatory markers, including TNF-α, Interleukin-1 beta (IL-1β), and Interleukin-18 (IL-18), as well as mRNA and protein expression of TLR4, NOX4, NLRP3, NF-κB, ASC, TNF-α, and Caspase-1 in the brain tissues of MCAO rat levels. Conclusion: STQJD effectively ameliorates IS in MCAO/R rats by modulating the NOX4/TLR4/NF-κB/TNF-α signaling pathway, reducing inflammation and oxidative damage, and exerting neuroprotective effects.

Keywords: Shu-Tiao Qi-Ji decoction, ischemic stroke, network pharmacology, NOX4/TLR4/NF-κB/TNF-α, Traditional Chinese Medicine

Introduction

A stroke, also known as an "acute cerebrovascular event", is a sudden-onset cerebrovascular disorder resulting from either a ruptured blood vessel or an obstruction of blood flow to brain tissue, leading to brain damage [1]. Stroke can be classified as hemorrhagic, ischemic, subarachnoid hemorrhage, or of undetermined type, with ischemic stroke (IS) representing over 75% of all cases [2]. Currently, the primary clinical treatments for IS include intravenous tissue plasminogen activator (tPA) administration, arterial thrombolysis, and endovascular thrombectomy [3-5]. However, their clinical application is often limited by challenges associated with IS treatment, including a narrow therapeutic time window, risk of hemorrhagic complications, and potential for reperfusion injury [6-8]. Accordingly, developing novel, safe, and effective therapies for IS are of great clinical importance [9].

Shu-Tiao Qi-Ji decoction (STQJD) was developed by Professor Zhang Zhen, a renowned master of Chinese medicine in China, by integrating

https://doi.org/10.62347/MLZI7617

clinical knowledge of medicine and advancements in research on qi dysregulation. STQJD, composed of Bupleurum chinense (Chaihu), Cyperus rotundus (Xiangfu), Angelica sinensis (Danggui), Astragalus membranaceus (Huangqi), Eucommia ulmoides (Duzhong), Salvia miltiorrhiza (Danshen), Ligusticum chuanxiong (Chuanxiong), Citrus aurantium (Zhishi), Paeonia lactiflora (Hangshao), Atractylodes macrocephala (Baizhu), Poria cocos (Fuling), Dioscorea opposita (Shanyao), and Glycyrrhiza uralensis (Sheng Gancao), has functions of promoting blood circulation, awakening the brain, soothing the liver, regulating Qi flow, and restoring Qi movement. However, its specific mechanism for treating IS requires further research. Previous studies have revealed that most active ingredients in STQJD protect against cerebral ischemia-reperfusion injury (CIRI) through multiple pathways. For instance, astragaloside IV has been demonstrated to reduce CIRI in the brain by preventing apoptosis via the P62/Keap1/Nrf2 signaling pathway [10]. Angelica extracts protect against CIRI by activating the p90RSK/p-Bad and p90RSK/CREB/BDNF signaling pathways, mediated by p38 MAPK, following global cerebral ischemia in rats [11].

Our previous clinical and experimental studies demonstrated that STQJD exerts a significant therapeutic effect on IS. However, the exact molecular mechanism remains unclear. In Traditional Chinese Medicine (TCM), the diagnosis and treatment of diseases depend on a thorough evaluation of their causes and progression, similar to precision medicine [12]. However, the multi-target, multi-effect, and multi-layered nature of herbal decoctions presents significant challenges in elucidating their mechanisms of action [13]. Network pharmacology is a discipline that combines systems biology and multidirectional pharmacology, offering researchers new strategies for drug development [14]. Its systematic, integrative, and precise characteristics make it ideal for investigating the pharmacological mechanisms of TCM formulations and for more intuitively illustrating the biological effects and potential molecular mechanisms of drugs acting on diseases [15].

Therefore, in this study, the results of preliminary clinical studies and network pharmacology prediction were combined to investigate the regulatory effects of serial concentrations of STQJD on the NOX4/TLR4/NF-κB/TNF-α signaling pathway and the effects of inflammatory factors in IS rats. Moreover, the molecular mechanism of STQJD's anti-IS activity was comprehensively investigated to provide a new perspective and laboratory data support for preventing and treating IS.

Materials and methods

Drugs preparation

STQJD: The clinical dosage of STQJD is 161 g of raw material/person/day. This was converted to an equivalent dose of 16.905 g/kg for the MCAO/R rat's medium dose based on body surface area. The low-dose and high-dose concentrations were set at 50% (8.453 g/kg) and 200% (33.810 g/kg) of the medium dose, respectively. A total of 1893.36 g of raw herbs were weighed according to the specified proportions (**Table 1**). Soaking procedure: The 1893.36 grams of herbs were rinsed with about 7.7 L of water for 1 to 2 hours. Boil and extraction: The soaked water, together with the herbs, was boiled and extracted twice, each time for 1 hour. Concentrations: After boiling and extracting twice, the drug residue was filtered through a metal funnel net, and the filtered drug solution was concentrated to about 600 mL to obtain a solution with a concentration of 3.381 g/mL (high dose) (The apparatus used for boiling and concentrating was a 300 sandwich pot manufactured by Zhejiang Shentai Special Equipment Product No.: R2015-0761). Dispensing: Dispense, as required, into the required amounts of bottles. Once cooled, the decoction was preserved at -80°C to ensure stability for subsequent experimental use. The low-dose (0.84525 g/mL) and medium-dose (1.6905 g/mL) solutions were prepared by diluting the high-dose solution. All herbal materials were sourced from the Preparation Center at Kunming Municipal Hospital of Traditional Chinese Medicine, adhering rigorously to the specifications outlined in the 2020 edition of the Chinese Pharmacopoeia.

Positive control drug (Nimodipine): Batch No: H20003010, purchased from Bayer Healthcare. Dosage: The drug specification is 30 mg/tablet, with two tablets dissolved in 54 mL of normal saline to prepare a 1.08 mg/mL nimodipine solution [16].

Table 1. Composition of Shu-Tiao Qi-Ji decoction

Chinese name	Latin name	Dose (g)	source
Chaihu	Bupleurum chinense	10 g	Yunnan Ningkun Biotechnology Co.
Xiangfu	Cyperus rotundus	10 g	Yunnan Zongshun Biotechnology Co.
Danggui	Angelica sinensis	15 g	Yunnan New Century Chinese Medicine Drinking Tablets Co.
Huangqi	Astragalus membranaceus	20 g	Yunnan Baiyao Group Chinese Medicine Resources Co.
Duzhong	Eucommia ulmoides	15 g	Yunnan Baiyao Group Chinese Medicine Resources Co.
Baizhu	Atractylodes macrocephala	10 g	Yunnan New Century Chinese Medicine Drinking Tablets Co.
Danshen	Salvia miltiorrhiza	10 g	Chengdu Kangmei Pharmaceutical Manufacturing Co.
Chuanxiong	Ligusticum chuanxiong	10 g	Yunnan Ningkun Biotechnology Co.
Zhishi	Citrus aurantium	10 g	Yunnan Tian Jiang Fang Fang Pharmaceutical Co.
Hangshao	Paeonia lactiflora	10 g	Yunnan New Century Chinese Medicine Drinking Tablets Co.
Shangyao	Dioscorea opposita	20 g	Yunnan Kern Pharmaceutical Drinking Tablets Co.
Sheng Gancao	Glycyrrhiza uralensis	6 g	Yunnan Baiyao Group Chinese Medicine Resources Co.
Fuling	Poria cocos	15 g	Yunnan Kern Pharmaceutical Drinking Tablets Co.

Animal study

Modeling and grouping: 150 SPF-grade healthy adult male SD rats, weight: 280 ± 20 g, from the Animal Division of Kunming Medical University (License No. SCXL [Dian] 2015-0002) were used for study. The rats were housed under specific conditions (temperature: 22.5 ± 2.5°C, humidity: 40%-70%) for one week with free access to food and water to allow acclimatization. Subsequently, we established a MCAO/R model using a modified Zea-Longa method. The rats were anesthetized via intraperitoneal injection of 3% sodium pentobarbital (0.3 mL/100 g) and secured in a supine position on a sterilized wooden board. A midline incision was made on the neck, carefully exposing the left internal carotid artery. A pre-treated suture was introduced into the artery through a distal incision until resistance was felt, indicating occlusion. After inducing ischemia for 1.5 hours, the suture was slowly pulled out to recover middle cerebral artery blood flow, and a ligature was applied to prevent hemorrhage. In the end, the incision was sutured. After the operation, the rats were assessed using the Zea-Longa scoring scale upon regaining consciousness. Only the rats with scores between 1 and 3 were stochastically assigned to experimental groups, while others were excluded. The successfully modeled rats were stochastically allocated into six groups: (1) Sham group; (2) MCAO/R group; (3) Low-dose STQJD group (8.453 g/kg); (4) Medium-dose STQJD group (16.905 g/kg); (5) High-dose STQJD group (33.81 g/kg); (6) Nimodipine group (10.8 mg/kg). All treatments were administered once daily via oral gavage at a consistent time for 14 days (1 mL/100 g). The Sham group and MCAO/R groups were given normal saline.

Sample preparation: Following the 14-day treatment period, the rats were fasted for 12 hours with free access to water before anesthesia was administered via intraperitoneal injection. Approximately 4 mL of blood was aseptically drawn from the abdominal aorta and centrifuged at 3,000 rpm for 15 minutes at 4°C to obtain serum. Following blood collection, brain tissues were immediately harvested. The serum and brain tissues were preserved at -80°C for subsequent analyses.

Euthanasia: The brain tissue collection in this study strictly adhered to international ethical standards. The standardized procedures were as follows: (1) Following AAALAC's principle of "anesthesia prior to euthanasia", deep anesthesia was induced via intraperitoneal injection of 3% pentobarbital sodium (0.3 mL/100 g body weight); (2) Euthanasia was humanely performed through cervical dislocation in accordance with the AVMA Guidelines for the Euthanasia of Animals (2020 Edition), with death confirmation by rapid decapitation using a rodent guillotine as specified in Article 8.3 of China's Guidelines for the Ethical Review of Laboratory Animal Welfare. Immediately after decapitation, brain tissues were dissected and flash-frozen in liquid nitrogen to optimally preserve molecular integrity for subsequent analyses. All experimental protocols were rigorously reviewed and approved by the Institutional Animal Care and Use Committee of Kun-

ming Medical University (Ethical Approval No.: Kmmu20231583), ensuring full compliance with international ethical standards.

Neurological function scoring

After the operation, when the rat fully regained consciousness, their neurological function was evaluated using the Zea-Longa scoring system. Rats scoring between 1 and 3 were included in our study and randomly divided into groups, while others were excluded. After two weeks of drug administration, neurological function was reassessed and recorded to evaluate the extent of neurological deficits in each group. The Zea-Longa scoring system is defined as follows [17]: 0 points: natural activity; 1 point: incomplete extension of the left forepaw upon tail suspension, inward rotation observed; 2 points: inability to walk straight, exhibiting leftward circling; 3 points: marked inability to walk straight, with leftward tilting; and 4 points: loss of spontaneous activity, unconsciousness, or even death.

TTC

After the 14-day treatment period, rats were anesthetized and decapitated quickly to ensure brain integrity. The brains were snap-frozen for 20 minutes in a low-temperature freezer, then sectioned into 5-6 slices, each approximately 2 mm thick. They were incubated in a 2% TTC solution for 10-15 minutes at 37°C, protected from light, and occasionally turned to ensure even staining. The stained sections were subsequently emersed in paraformaldehyde for 24 hours before photographing. The cerebral infarct area was quantified using ImageJ 6.0 software.

Hematoxylin-eosin

Brain tissues were fixed using paraformaldehyde for 24 hours, then dehydrated, embedded in paraffin, and sliced (5 μm thickness). HE staining was applied, and pathological changes in the cortical and hippocampal regions were subsequently examined under a microscope for each group.

Nissl staining

Each section was stained by dewaxing, hydration, and a 1% toluidine blue solution. After washing in running tap water, tissue was submerged into 80%, 90%, and 95% alcohol, dehydrated, cleared, and finally sealed with neutral resin. Changes in Nissl bodies in the cortical and hippocampal regions were subsequently examined under a microscope for each group.

TUNEL staining

TUNEL staining was carried out following the protocol outlined in the instruction manual of the TUNEL kit (Beyotime Biotechnology Co., Ltd.). Apoptotic cells in the cortical and hippocampal regions were visualized using a fluorescence microscope (Leica, Germany) to assess the neuronal apoptosis of each drug-treated group.

Collection of active components and targets of STQJD

The active ingredients in the 13 herbs in STQJD were screened using the TCMSP and BATMAN-TCM. For the TCMSP, screening criteria included an OB ≥ 30%, DL ≥ 0.18, and BBB ≥ -0.3, while for BATMAN-TCM, with the prediction score cutoff > 20. Potential targets of STQJD's active compounds were retrieved from the Uniprot by searching for protein names and limiting the species to Humans.

Collection of stroke-related targets

Cerebral ischemic stroke-related target was obtained from the OMIM and GeneCards databases using "cerebral ischemic stroke" as the keyword. Duplicate targets were excluded.

PPI network construction

Drug ingredient targets and disease-related targets were input into Venny2.1.0 to generate Venn diagrams. After the STRING established the PPI network, the interaction data were visualized in Cytoscape 3.7.1 to identify protein interactions.

STQJD herb-active ingredient-target network

We imported the drug-active ingredient-target relationship file into Cytoscape version 3.7.1 to construct a network diagram depicting the relationships between STQJD herbs, their active ingredients, and their targets.

Table 2. qRT-PCR primer design

Gene	Primers	Product length (bp)
GAPDH	F: GGCAAGTTCAACGGCACAGTC	21
	R: TCGCTCCTGGAAGATGGTGATG	22
NOX4	F: CCTTTGTGCCTATACTGTGCTGAG	24
	R: CATACGGAGTTCCATGACATCTGAG	25
NF-κB	F: CGGTTACGGGAGATGTGAAGATG	23
	R: GAAGGTGGATGATGGCTAAGTGTAG	25
TNF-α	F: GCCCAGACCCTCACACTCAG	20
	R: CCGCTTGGTGGTTTGCTACG	20
NLRP3	F: TGGACCTCAACAGACGCTACAC	22
	R: GTCCTGCCAATGGTCAAGAGTTC	23
ASC	F: ATGGAAGAGTCTGGAGCTGTGG	22
	R: AATGAGTGCTTGCCTGTGTTGG	22
Caspase-1	F: GATGTTGACCTCAGAGAAATGAAGTTG	27
	R: TGGGCAGGCAGCAAATTCTTTC	22
TLR4	F: CTATCATCAGTGTATCGGTGGTCAG	25
	R: TTACAGCCAGCAATAAGTATCAGGTG	26

GO and KEGG enrichment analysis

To categorize a large number of genes according to their participation in biological processes, molecular functions, and cellular components, GO enrichment analysis was performed using the Metascape online database with the setting 'Homo sapiens'. Similarly, to further explore the role of STQJD active ingredients in specific signaling pathways, drug-disease common targets were uploaded to DAVD for KEGG analysis. The results of GO and KEGG analyses were visualized using bar charts and bubble plots.

Kit testing

The levels of ROS (Shanghai Meilian Biotechnology Co., Ltd.), TNF-α, IL-1β, and IL-18 (Shanghai Jianglai Biotechnology Co., Ltd.) in rat serum were quantified by available kits.

RT-qPCR

RNA was isolated from rat brain tissue using Trizol (Thermo Fisher Scientific, Cat. No.: 15596026CN). First-strand cDNA was synthesized via reverse transcription, with 2 μg RNA as the input, following the protocol provided by the FastKing RT Kit with gDNase (Thermo, Cat. No.: K1622). Quantitative PCR (qPCR) was subsequently performed to assess the relative mRNA expression levels of NOX4, NF-κB, TLR4, TNF-α, NLRP3, ASC, and Caspase-1, using a qPCR kit from Roche (Cat. No.: 04913914001). GAPDH served as the internal reference gene, and the primer was synthesized by Sangon Biotech (see **Table 2** for sequences). Gene expression analysis was carried out using the $2^{-\Delta\Delta Ct}$ method.

Western blotting

Protein was extracted from rat brain tissue previously frozen in -80°C freezer, washed with PBS, and lysed with 100 μL of RIPA lysate and enhanced protease inhibitor (100:1 prepared in advance) per 30 μg of brain tissue. Protein concentration was measured using the BCA kit (WAN Bioscience and Technology: WLA019a). After adding the corresponding amount of sample loading buffer to the protein samples, the samples were denatured by boiling at 100°C for 10 minutes. The proteins were separated via SDS-PAGE, then transferred onto PVDF membranes, sealed with 5% skim milk for 2 hours and incubated overnight at 4°C with primary antibodies targeting β-actin (Proteintech, 66009-1-Ig), NF-κB (Abmart, T55034S), phospho-NF-κB (Abmart, TP56372S), TLR4 (ABclonal, A5258), NLRP3 (ABclonal, A5652), ASC (ABclonal, A22046), NOX4 (Proteintech, 14347-1-AP), Caspase-1 (ABclonal, A0964), GAPDH (Proteintech, 10494-1-AP), and TNF-α (Bioss, bs-10802R). The following day, membranes were rinsed and incubated with HRP-conjugated secondary antibodies (anti-rabbit or anti-mouse IgG, Proteintech, SA00001-2/SA00001-1) for 2 hours. Finally, a chemiluminescent substrate was used to visualize the antibody binding. Protein quantification was performed with ImageJ software, normalizing protein expression to the internal reference GAPDH or β-actin, calculated as the ratio of the target protein's gray value to the reference.

Immunofluorescence

Upon completion of sectioning, tissue was first sealed with goat serum for 1 hour, followed by incubation at 4°C for 24 hours with primary antibodies against TNF-α and NF-κB. The next

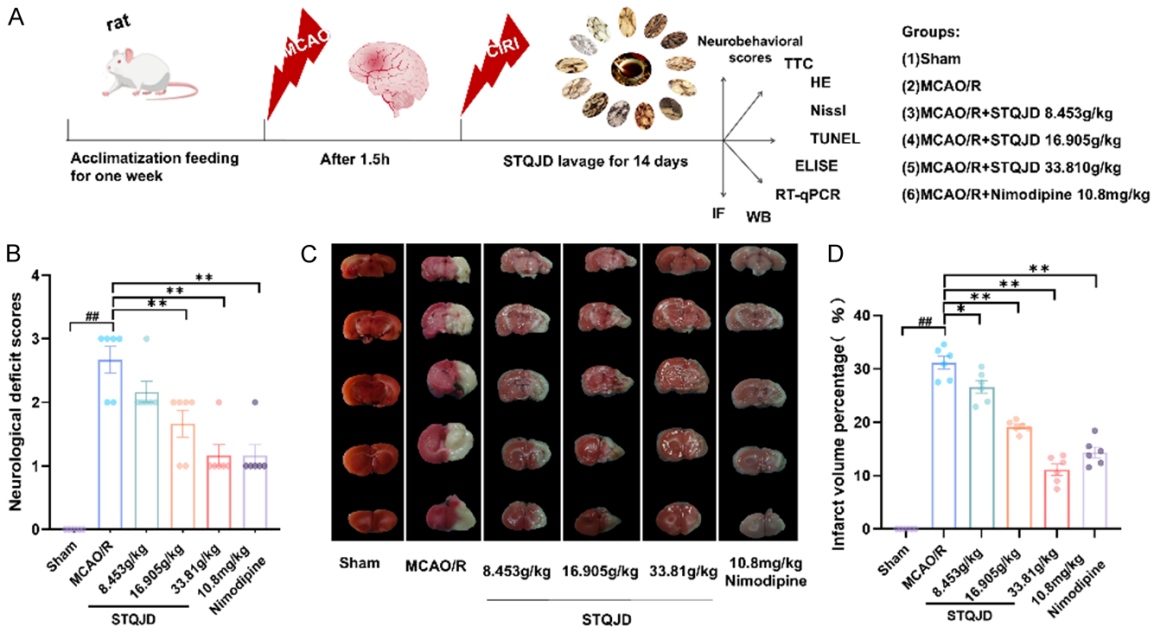

Figure 1. Animal experimental design and the effect of STQJD on MCAO/R-induced injury in rats. A. Animal experimental design. B. Neurological function scores. C. Infarct area. D. Infarct volume statistics Data are presented as mean ± SEM (n = 6). ##P < 0.01 versus the Sham group; *P < 0.05, **P < 0.01 versus the MCAO/R model group.

day, the sections were rinsed three times in PBS, each wash lasting 5 minutes, incubated with HRP-labeled anti-rabbit secondary antibody for 1 hour. After three additional 5-minute PBS washes, DAPI (Beyotime) was applied for 5 minutes to counterstain nuclei, and the sections were mounted using an anti-fluorescent sealing solution. Finally, Fluorescence imaging was conducted with a fluorescence microscope.

Statistical analysis

Statistical analyses were conducted with GraphPad Prism 8.0, presenting data as mean ± SEM; for comparisons between the two groups, an unpaired t-test was utilized, whereas one-way ANOVA was employed to assess differences across multiple groups. Statistical significance was defined as a *p*-value below 0.05.

Results

Neurological Function scores and infarct area

Compared with the Sham group, the neurological scores in the MCAO/R group were significantly increased (P < 0.01), indicating impaired neurological function. However, treatment with medium- and high-dose STQJD as well as nimodipine significantly reduced neurological scores compared with the MCAO/R group (P < 0.01) (**Figure 1B**). Regarding cerebral infarction, the Sham group displayed no infarct, while the MCAO/R group developed significant infarct areas, confirming successful modeling (P < 0.01). After 14 days of treatment, compared with the MCAO/R group, all STQJD groups demonstrated a decrease in the cerebral infarct area, and the high-dose STQJD group exhibiting the most significant reduction (P < 0.01) (**Figure 1C**, **1D**). These results indicate that STQJD can improve neurological function and reduce cerebral infarction in IS rats.

STQJD improves pathological damage in MCAO/R rat brain tissue

HE staining was performed to assess the neuroprotective effects of STQJD on cortical and hippocampal neuronal damage in MCAO/R rats (**Figure 2**). Neurons in the Sham group displayed typical morphology, with a standard structure and orderly arrangement. In contrast, the MCAO/R group demonstrated significant pathological changes, including tissue loosening, edema, vacuolar degeneration, neuronal disorganization, demyelination, and prominent

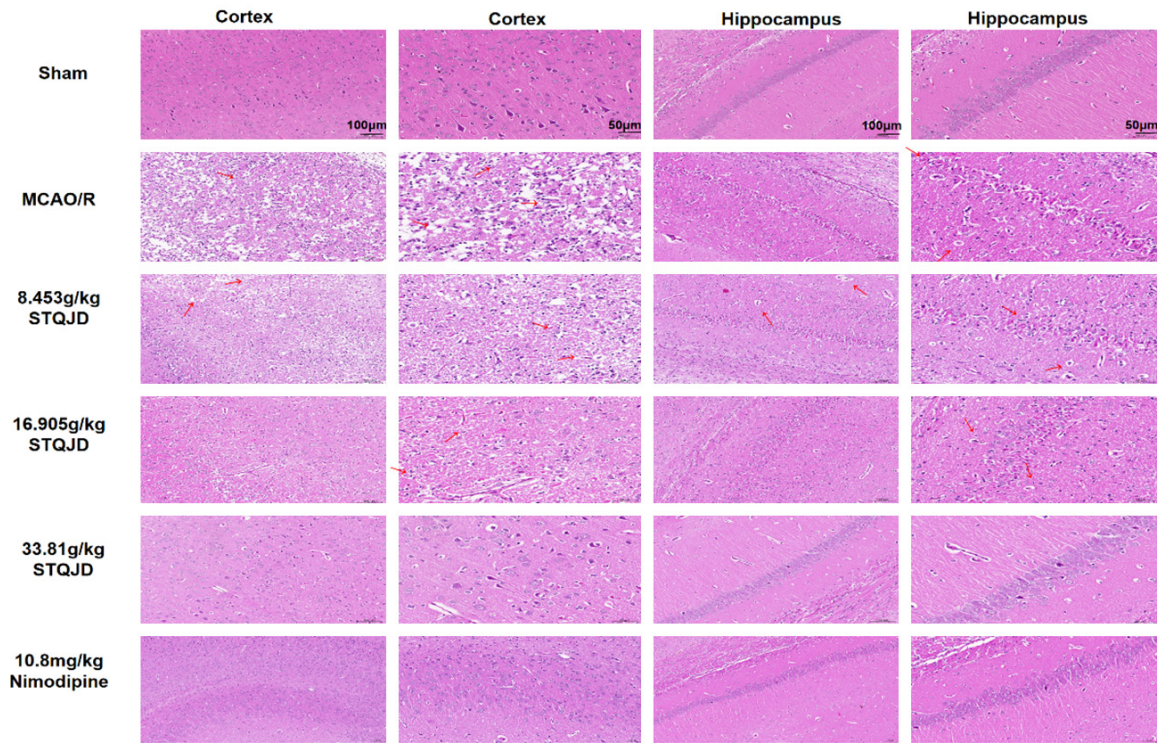

Figure 2. STQJD reduces pathological damage caused by MCAO/R. HE staining was performed to assess the impact of STQJD on neuronal damage within the cortical and hippocampal regions of MCAO/R rats (n = 3, 100×, scale bar = 100 μm; 200×, scale bar = 50 μm).

inflammatory cell infiltration. Following the 14-day treatment period, the low- and medium-dose STQJD groups showed slight improvements in tissue loosening and edema. In contrast, the high-dose STQJD and nimodipine groups exhibited neuronal morphology closer to normal, with orderly cell arrangement compared to the MCAO/R group. These findings indicate that STQJD mitigates neuronal damage and promotes structural recovery in the brain tissue of ischemic stroke rats.

STQJD reduces neuronal damage in MCAO/R rat brain tissue

Nissl bodies are primarily located in neuronal cell bodies and dendrites, and their reduction or disappearance serves as a marker of neuronal injury [18]. In the Sham group, neuronal cells were tightly arranged and exhibited large, deep-blue Nissl bodies along with a high cell count. Conversely, the MCAO/R group was severely damaged, characterized by lighter Nissl body staining, disintegration, and disappearance ($P < 0.01$). Following the 14-day treatment period, compared with the MCAO/R group, the medium- and high-dose STQJD groups, as well as the nimodipine group, showed significant improvements in neuronal morphology, including more complete Nissl bodies and increased number of surviving neurons ($P < 0.01$) (**Figure 3A-C**). These findings indicate that STQJD attenuates neuronal damage in IS rat brain tissue.

STQJD reduces neuronal apoptosis caused by ischemia

After 14 days of drug administration, TUNEL staining was used to evaluate neuronal apoptosis in rat brain tissue (**Figure 3D-F**). No apoptotic cells (red fluorescence) were observed in the Sham group. Conversely, the MCAO/R group displayed many apoptotic cells in the cortex and hippocampus ($P < 0.01$). The medium- and high-dose STQJD groups and the nimodipine group showed a significant reduction in neuronal apoptosis Compared with the MCAO/R group after 14 days of administration ($P < 0.01$). These results suggest that STQJD significantly attenuates ischemia-induced neuronal apoptosis.

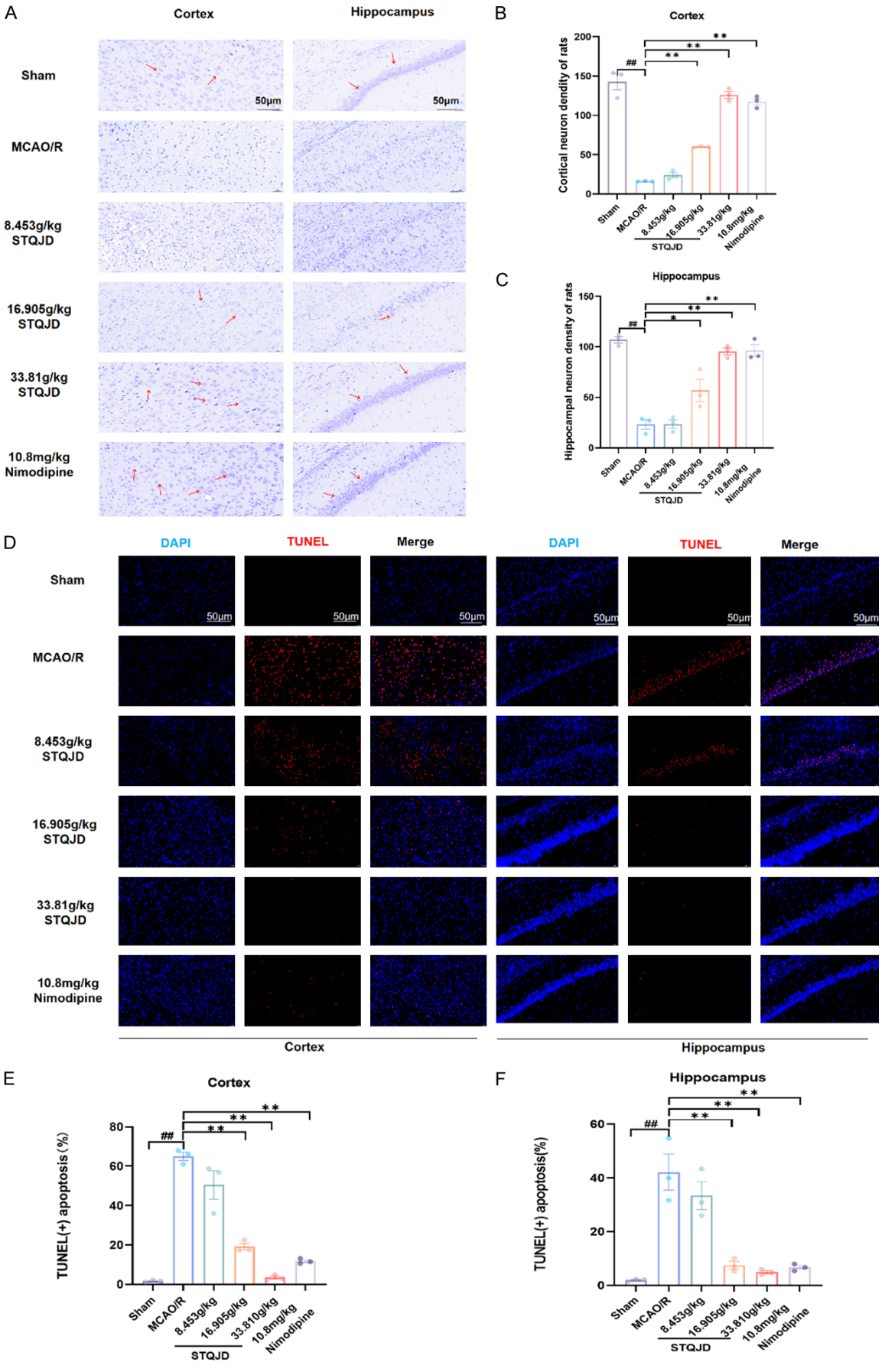
A
Cortex
Hippocampus
Sham
MCAO/R
8.453g/kg STQJD
16.905g/kg STQJD
33.81g/kg STQJD
10.8mg/kg Nimodipine
50μm
B
Cortex
Cortical neuron density of rats
C
Hippocampus
Hippocampal neuron density of rats
Sham
MCAO/R
8.453g/kg
16.905g/kg
33.81g/kg
10.8mg/kg Nimodipine
STQJD
D
DAPI
TUNEL
Merge
Cortex
Hippocampus
E
Cortex
TUNEL(+) apoptosis (%)
F
Hippocampus
TUNEL(+) apoptosis(%)

Figure 3. Effects of STQJD on Nissl body and neuronal apoptosis in rats with MCAO/R injury. A. Effects of STQJD on Nissl body changes in cortical and hippocampal regions (200×, scale bar = 50 μm). B. Number of Nissl corpuscles in the cortical area. C. Number of Nissl corpuscles in the hippocampus. D. Impact of STQJD on neuronal apoptosis in the cortex and hippocampal regions (200×, scale bar = 50 μm). E. Changes in the neuronal apoptosis index in the cortical region. F. Changes in the neuronal apoptosis index in the hippocampal region. Data are presented as mean ± SEM (n = 3). $^{\#\#}P < 0.01$ versus the Sham group; $^{*}P < 0.05$, $^{**}P < 0.01$ versus the MCAO/R model group.

Common targets between STQJD and IS

Using TCMSP and BATMAN-TCM databases, 239 active ingredients of STQJD were obtained. After correcting gene names using the UniProt database and the removal of duplicates, 280 component targets of STQJD were obtained. Through searches of the OMIM and GeneCards databases with the keyword "cerebral ischemic stroke", 1,788 disease-related targets were identified. Of these, 151 targets were found to be shared between the drug and the disease (**Figure 4A**).

PPI

To better understand STQJD's mechanism, we used the String and set an organism as "Homo sapiens" with confidence > 0.900 to get the PPI network. The result comprised 126 nodes and 321 interactions. In this network, nodes are scaled and shaded according to the number of interactions they have, with larger and darker nodes indicating more excellent connectivity. Edges represent interactions between proteins, with thicker and darker edges reflecting stronger associations between proteins (**Figure 4B**, **4C**).

STQJD herb-active component-target network

To better understand the roles of individual components of STQJD in ischemic stroke, the drug-active component-target interaction file is imported into cytoscape 3.7.1 to construct a network diagram of STQJD's each drug, active component-target (**Figure 4D**). This diagram includes 533 nodes and 5,469 edges. The color intensity and size of node correlate with the significance of each compound's role, with larger and more intensely colored nodes indicating higher importance. The top 10 key components of STQJD, along with their corresponding herbs, are listed in **Table 3**.

GO and KEGG enrichment analysis

In the GO enrichment analysis, the top three enriched GO-BP items were senescence, exogenous apoptotic, and cell response to chemical stress. The most enriched terms for GO-CC included platelet alpha granule lumen, secretory granule lumen, and platelet alpha granule. For GO-MF, the most significant terms were DNA-binding transcription factor binding, RNA polymerase II-specific DNA-binding transcription factor binding, and cytokine activity (**Figure 5A**, **5B**). KEGG analysis was performed on 151 key targets through the DAVID database and identified 208 pathways. The key enriched pathways included fluid shear stress atherosclerosis signaling pathway and TNF / IL-17 signaling pathway (**Figure 5C**, **5D**). The key signaling pathway map was displayed (**Figure 5E**).

Effects of STQJD on ROS and inflammatory cytokine levels in MCAO/R rats

ROS are a source of oxidative stress and are by-products of oxygen metabolism, playing a critical role in the onset and progression of IS. During IS, ROS can mediate inflammation cascades by increasing the expression of inflammatory mediators like TNF-α, IL-1β, and IL-18, thereby exacerbating brain tissue damage [18]. Compared with the Sham group, the Kit test results revealed that IL-18, ROS, IL-1β, and TNF-α levels in the MCAO/R group were significantly elevated ($P < 0.01$). Conversely, compared with the MCAO/R group, in the medium- and high-dose STQJD treatment groups significantly decreased these inflammatory markers ($P < 0.01$) (**Figure 6A-D**). These results indicate that STQJD possesses anti-inflammatory effects and may alleviate ROS-mediated damage in IS.

Target gene mRNA levels

RT-qPCR was employed to assess the mRNA expression levels of NF-κB, NOX4, TLR4, NLRP3, ASC, TNF-α, and Caspase-1 in rat brain tissues. Compared with the Sham group, the MCAO/R group exhibited significantly increased expression of these genes-NOX4, NF-κB, TLR4, TNF-α, NLRP3, ASC, and Caspase-1 were dramatically elevated ($P < 0.01$). Following the

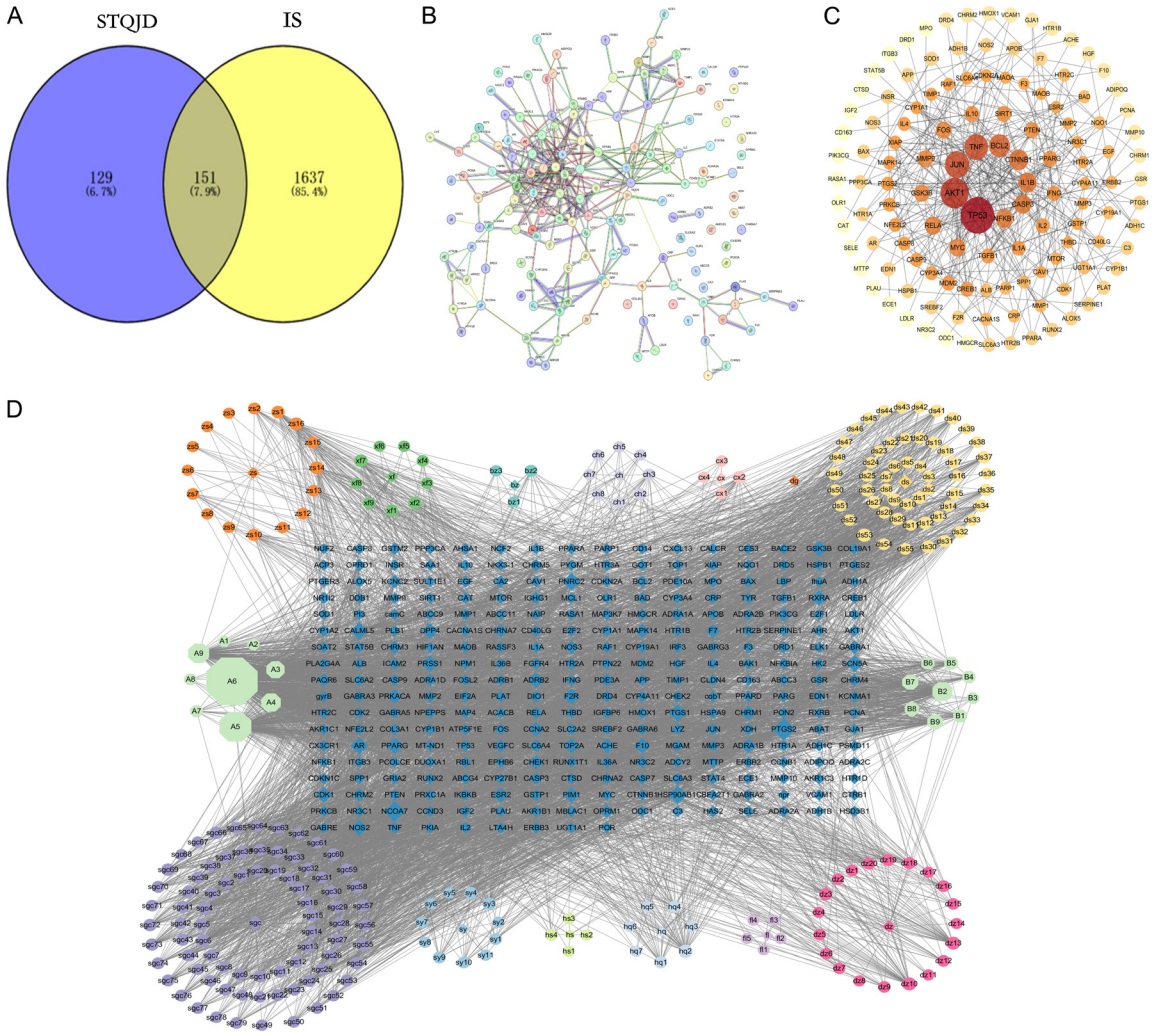

Figure 4. Common targets between STQJD and IS and ingredients -Target-disease Network diagram. (A) Common targets between STQJD and IS (B) PPI network diagram. (C) Visualization of the PPI network. (D) STQJD Herb-Active Ingredients-Target Network diagram.

14-day treatment period, compared with the MCAO/R group, all STQJD-treated groups showed a dose-dependent downregulation of these inflammatory markers ($P < 0.05$; $P < 0.01$) (**Figure 6E-K**). These results suggest that STQJD may offer neuroprotection in IS by regulating the NOX4/TLR4/NF-κB/TNF-α pathway, thereby attenuating inflammation and oxidative stress in neurons.

Expression of target proteins

Compared with the Sham group, Western blot analysis indicated the protein expression in the MCAO/R group of TLR4, NOX4, NF-κB, NLRP3, ASC, TNF-α, and Caspase-1 were dramatically increased ($P < 0.01$). After 14 days of treatment, compared with the MCAO/R group, STQJD administration significantly attenuated these abnormally elevated protein levels ($P < 0.05$; $P < 0.01$) (**Figure 7A-G**). These results suggest that STQJD may offer neuroprotection against IS by modulating the NOX4/TLR4/NF-κB/TNF-α pathway, thereby alleviating inflammation and oxidative stress in neurons.

Immunofluorescence detection of TNF-α protein expression

Compared with the Sham group, Immunofluorescence analysis demonstrated that TNF-α and NF-κB expression levels in the cerebral cortex were dramatically increased in the MCAO/R group ($P < 0.01$). Following 14 days of treat-

Table 3. The first 10 key ingredients of Shu-Tiao Qi-Ji decoction

No.	MOL_ID	Key Component Name	Source Herb(s)	Degree
1	MOL000098	quercetin	Bupleurum, Eucommia, Astragalus, Raw Licorice, Cyperus rotundus	754
2	MOL000422	kaempferol	Bupleurum, Eucommia, Astragalus, Raw Licorice, Cyperus rotundus, Paeonia	383
3	MOL000006	luteolin	Salvia, Cyperus rotundus, Aurantium	174
4	MOL000358	beta-sitosterol	Angelica, Eucommia, Cyperus rotundus, Paeonia	156
5	MOL000354	isorhamnetin	Bupleurum, Astragalus, Raw Licorice, Cyperus rotundus	147
6	MOL000449	Stigmasterol	Bupleurum, Angelica, Dioscorea, Cyperus rotundus	120
7	MOL000392	formononetin	Astragalus, Raw Licorice	79
8	MOL004328	Naringenin	Aurantium, Raw Licorice	73
9	MOL000378	7-O-methylisomucronulatol	Astragalus	46
10	MOL000417	Calycosin	Astragalus, Raw Licorice	46

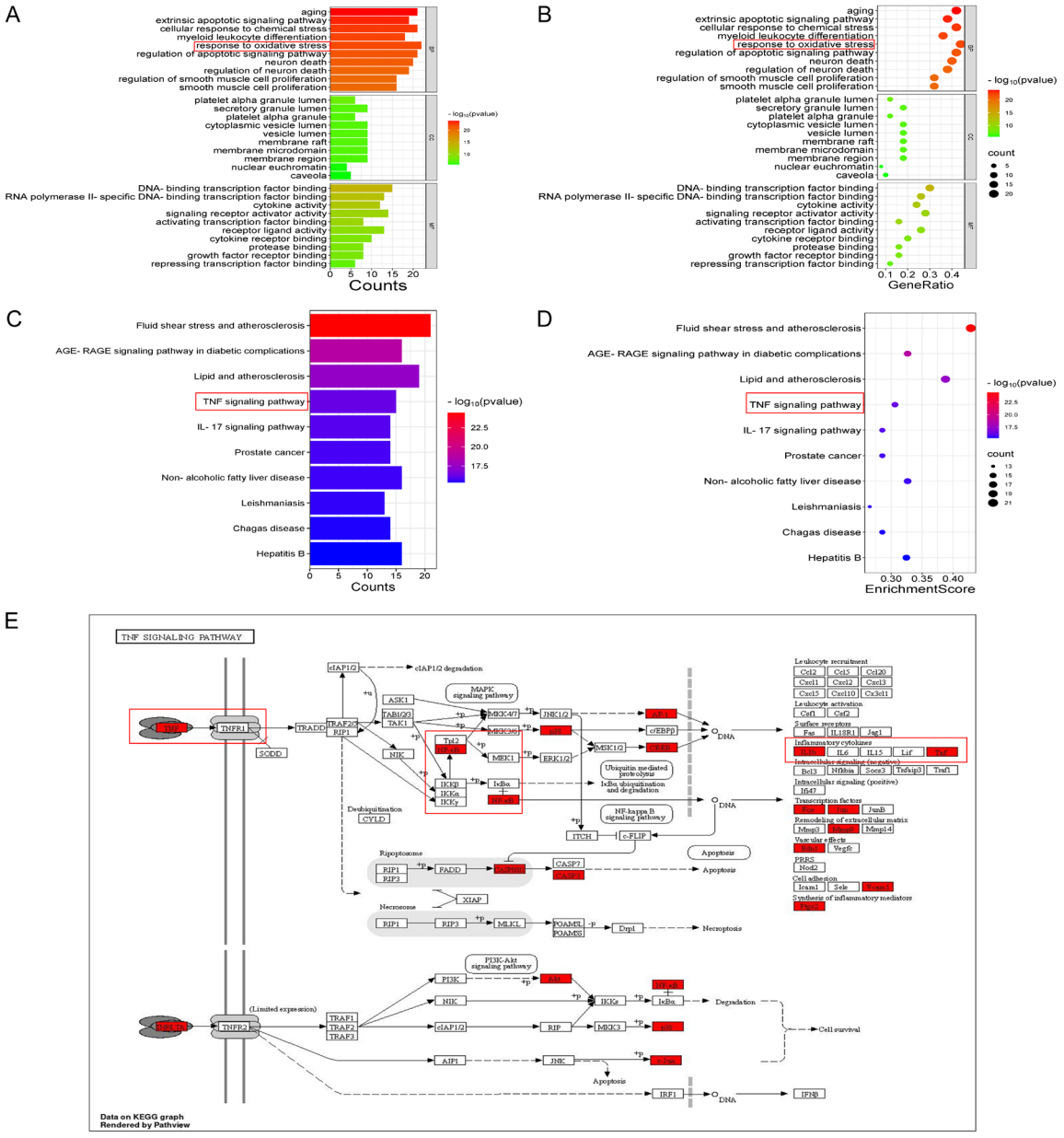

Figure 5. Enrichment analysis and molecular docking of key targets. A. GO bar chart. B. GO bubble chart. C. KEGG analysis top 10 pathways bar chart. D. KEGG analysis top 10 pathways bubble chart. E. TNF-α signaling pathway map.

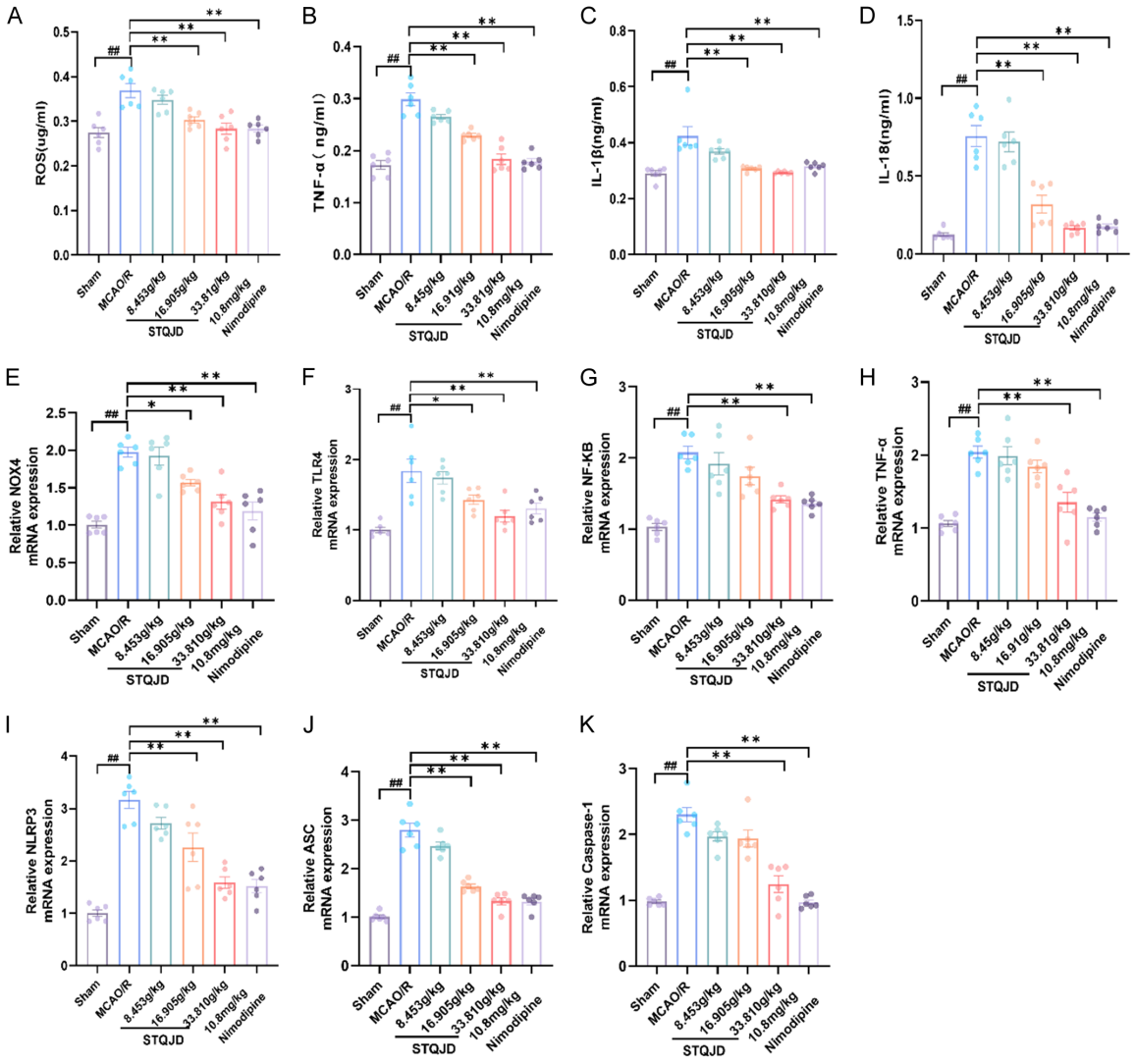

Figure 6. Effects of STQJD on ROS, inflammatory cytokine levels and NOX4/TLR4/NF-κB/TNF-α signaling pathway mRNA expression levels in MCAO/R rats. A. ROS. B. TNF-α. C. IL-1β. D. IL-18. E. NOX4. F. TLR4. G. NF-κB. H. TNF-α. I. NLRP3. J. ASC. K. Caspase-1. The $2^{-\Delta\Delta Ct}$ method was used to analyze the Q-PCR results. Data are presented as mean ± SEM (n = 6). $^{\#\#}P < 0.01$ versus the Sham group; $^{*}P < 0.05$, $^{**}P < 0.01$ versus the MCAO/R model group.

ment, compared with the MCAO/R group, both TNF-α and NF-κB expression were significantly reduced in the medium- and high-dose STQJD and the nimodipine group ($P < 0.01$) (**Figure 8A-D**).

Discussion

Shu-Tiao Qi-Ji Decoction (STQJD) can improve neurological deficits in patients by modulating Qi and blood, promoting cerebral blood circulation, and aiding in the restoration of blood supply to ischemic brain regions, thereby alleviating symptoms such as hemiplegia and speech impairments. However, the precise therapeutic mechanisms of STQJD in ischemic stroke (IS) remain unclear. It is often accompanied by severe inflammatory responses, brain tissue necrosis, and focal neuronal death and defects during IS [19, 20]. In this study, the therapeutic effects of STQJD on IS were evaluated by establishing a middle cerebral artery occlusion/reperfusion (MCAO/R) rat model and administering the treatment via oral gavage for 14 days. The results revealed that STQJD significantly improved neurological performance scores, decreased cerebral infarct size, decreased Nissl body loss, and attenuated neuronal apoptosis in rats (**Figures 1-3**). These find-

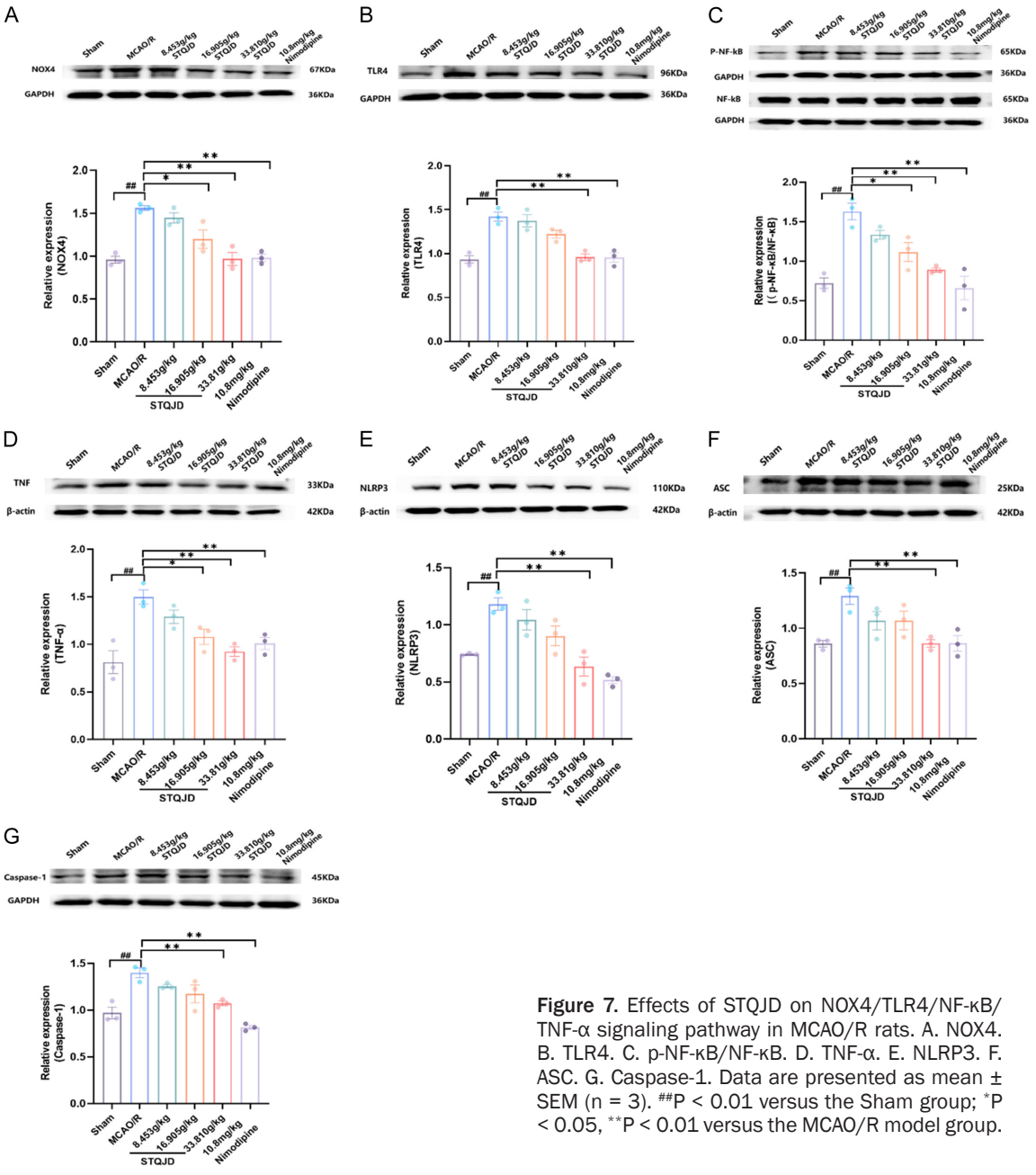

Figure 7. Effects of STQJD on NOX4/TLR4/NF-κB/TNF-α signaling pathway in MCAO/R rats. A. NOX4. B. TLR4. C. p-NF-κB/NF-κB. D. TNF-α. E. NLRP3. F. ASC. G. Caspase-1. Data are presented as mean ± SEM (n = 3). $^{\#\#}P < 0.01$ versus the Sham group; $^{*}P < 0.05$, $^{**}P < 0.01$ versus the MCAO/R model group.

ings indicate that STQJD provides a neuroprotective advantage in IS.

Given the complex, multi-target, and multifaceted nature of TCM formulations, such as STQJD, which complicates the elucidation of their mechanisms of action, a network pharmacology approach was used in this study to investigate the molecular mechanisms underlying STQJD's therapeutic effects in IS. After searching various Chinese medicine databases and relevant literature, 239 active components associated with STQJD were identified, with most exhibiting promising bioactivity. For instance, kaempferol (3,5,7,4'-tetrahydroxyflavone), a flavonol isolated from plants such as ginger, is present in several STQJD herbs, including Bupleurum, Eucommia, Astragalus, Licorice, Cyperus, and Paeonia. It can modulate post-stroke apoptosis, ferroptosis, and neuroinflammation, possibly through pathways such as the BDNF-TrkB-PI3K/AKT, Nrf2/SLC7A11/GPX4, and JAK1/STAT3 signaling [21, 22]. Luteolin, a flavonoid widely present in

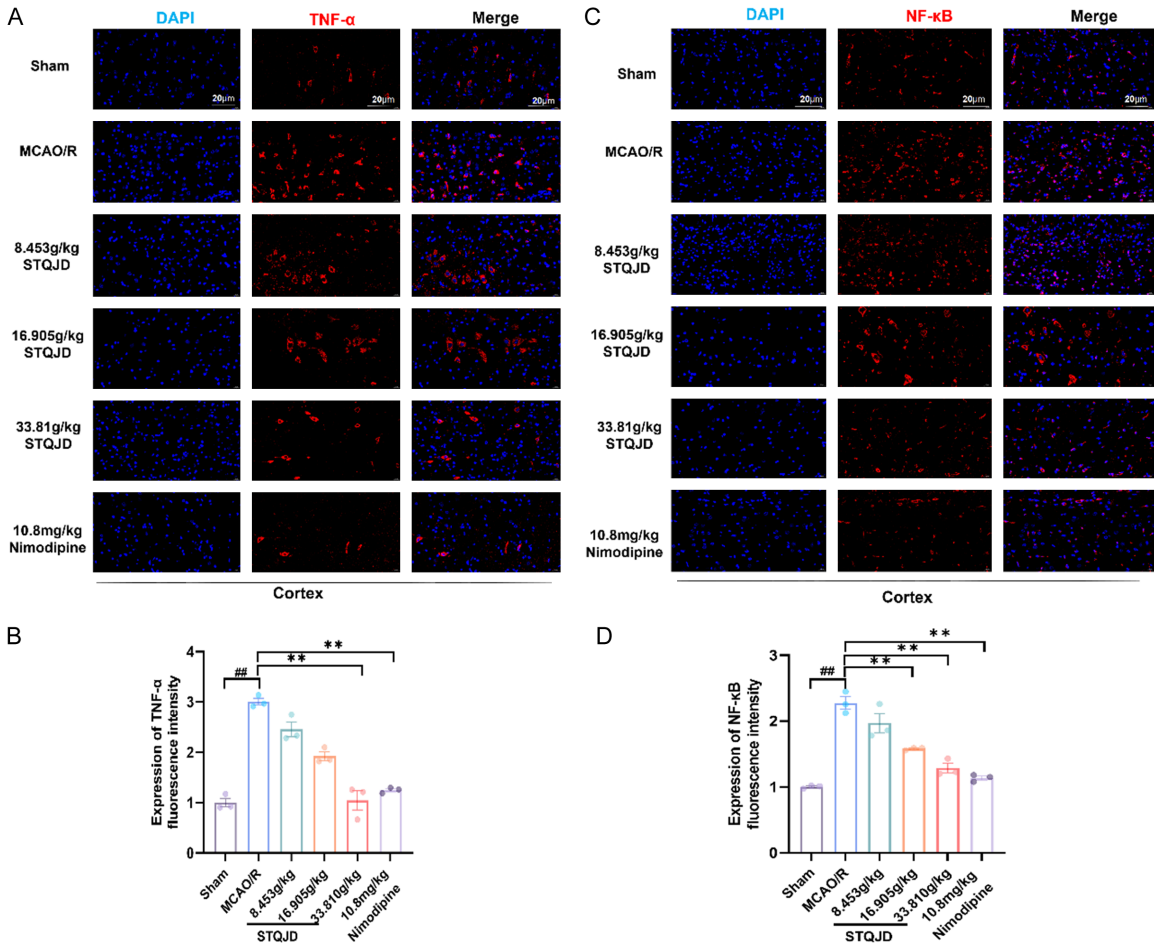

Figure 8. Effects of STQJD on NF-κB and TNF-α in MCAO/R rats. A. Immunofluorescence picture of TNF-α in the cortical region (400×, scale bar = 20 μm). B. Quantification of TNF-α. C. Immunofluorescence picture of NF-κB in the cortical region (400×, scale bar = 20 μm). D. Quantification of NF-κB. Data are presented as mean ± SEM (n = 3). ##P < 0.01 versus the Sham group; **P < 0.01 versus the MCAO/R model group.

numerous plants, exhibits potent anti-inflammatory, antioxidant, antiviral, and antiproliferative properties. It has demonstrated significant antioxidant activity and the ability to improve microcirculation in ischemia-reperfusion injury models [23-25]. β-Sitosterol, a plant sterol structurally similar to cholesterol, possesses significant antioxidant, lipid-lowering, anti-inflammatory, and anticancer properties in the central nervous system [26]. In a MCAO-induced IS mouse model, β-sitosterol reduced neuronal apoptosis and alleviated neurological deficits [27].

Furthermore, GO and KEGG analyses revealed that STQJD's anti-IS effects are strongly linked to inflammation, apoptosis, and oxidative stress pathways. In the protein-protein interaction network analysis, inflammation-related proteins (TNF-α, IL-1β, and MMP9), apoptosis-related proteins (Bcl-2, Caspase-3, and Bax), and oxidative stress-related proteins (AKT-1, Jun, and MAPK14) exhibited high degree values, indicating that they may serve as core targets for STQJD in treating IS. Fluid shear stress, atherosclerosis signaling pathways, and TNF and IL-17 signaling pathways were identified as critical pathways (**Figure 5**). In summary, the network pharmacology results provide a molecular basis and direction for investigating STQJD's therapeutic potential in IS. We hypothesized that STQJD exerts anti-IS effects through the TNF signaling pathway, which was confirmed by in vivo experiments.

During IS, brain damage may occur due to ROS overproduction and an imbalance between excessive ROS production and the antioxidant

defense system [28]. NADPH oxidase (NOX) is the only family of enzymes known to exhibit a single function for producing ROS, and NOX4 is one of the most extensively distributed NOX subtypes in the central nervous system [29]. The NOX4 gene encodes four protein variants: NOX4B, NOX4C, NOX4D, and NOX4E, with the functionally active NOX4D associated with ROS production [30, 31]. Our results demonstrated that STQJD reduced MCAO/R-induced NOX4 and ROS production, indicating that STQJD may prevent oxidative stress-induced ischemic brain injury (**Figures 6A**, **6E** and **7A**).

ROS production can further mediate the onset of associated inflammatory cascades during IS [32]. TLRs, a group of transmembrane pattern recognition receptors, play a critical role in initiating and regulating the inflammatory response during IS [33]. Among these, toll-like receptor 4 (TLR4) is particularly important as it activates NF-κB, leading to the overproduction of proinflammatory cytokines, a process that plays a central role in IS pathology [34]. Inhibiting the TLR4/NF-κB signaling pathway can protect the brain from neural damage in IS rats [35]. NF-κB functions as a transcription factor that controls the expression of various genes, including five family members: p50/p105 (NF-κB1), p65 (RelA), c-Rel, RelB, and p52/p100 (NF-κB2) [36]. In its resting state, NF-κB homodimers or heterodimers bind to the inhibitory protein I-κB, masking their nuclear localization signals and sequestering them in the cytoplasm [37]. I-κB kinase is activated by external stimuli (for example, bacterial or viral infection, inflammatory cytokines, ionizing radiation), leading to the phosphorylation and degradation of I-κB, and NF-κB is released for nuclear translocation and controlling the expression of inflammation-related genes, including TNF-α, IL-1β, IL-6, and NLRP3 [38-40].

NLRP3 is a complex composed of the NLRP3 protein, ASC, and caspase-1, which is highly expressed in neurons and immune cells [41]. Following IS, excessive formation of the NLRP3 inflammasome catalyzes caspase-1, which cleaves pro-IL-18 and pro-IL-1β into their active proinflammatory forms, IL-1β and IL-18 [42]. Additionally, this complex promotes the release of proinflammatory molecules within cells, leading to membrane rupture and further damage [43]. Our findings demonstrate that STQJD reduced the levels of NF-κB, NOX4, TLR4, NLRP3, ASC, TNF-α, and caspase-1 in the MCAO/R model, indicating that STQJD's neuroprotective effects in IS are partially mediated by modulation of the TLR4/NF-κB/TNF-α signaling pathway (**Figures 6B-D**, **6F-K**, **7B-G** and **8A-D**). The in vivo experimental results were consistent with the network pharmacology findings, validating the reliability of the network pharmacological results and elucidating the mechanisms by which STQJD treats IS.

This study provides theoretical and experimental basis for clinical application in the treatment of ischemic stroke. It further supports the potential application value of STQJD in the treatment of CIRI. However, this study still has some limitations. Although network pharmacology was employed to investigate the effects of STQJD in IS, compounds or targets that have not been identified and documented may not have been included in our analyses. Quercetin, kaempferol, and luteolin were identified in our studies as the first three most critical bioactive ingredients of STQJD for treating IS. Still, they may not fully encompass the therapeutic potential of STQJD. Furthermore, some of our findings have limited prior research support. As the roles and mechanisms of these potential active components in IS remain unexplained and unvalidated, we believe future research holds significant promise and value.

Conclusion

STQJD effectively ameliorates IS in MCAO/R rats by modulating the NOX4/TLR4/NF-κB/TNF-α signaling pathway, reducing inflammation and oxidative damage, and exerting neuroprotective effects.

Acknowledgements

Our research work was supported by the National Natural Science Foundation of China [82360088], the Applied Basic Research Joint Project of Yunnan Province Science and Technology Department and Kunming Medical University [202201AY070001-001], and Yunnan Provincial Basic Research Program [202501AY070001-141], and Yunnan Provincial Department of Education project [2024J0155], and Yunnan Undergraduate Education and Teaching Reform Research Project [JG2023001], Yunnan Provincial Science and

Technology Department-Applied Basic Research Joint Special Funds of Chinese Medicine [202101AZ070001-127, 202401AZ070001-065], Yunnan Provincial Key Laboratory of Pharmacology for Natural Medicines Open Fund Project [YKLPNP-G2506], and Kunming Medical University Talent Introduction Scientific Research Special Project [K132310536].

Disclosure of conflict of interest

None.

Address correspondence to: Sijin He and Lihua Gu, Department of Rehabilitation, Kunming Municipal Hospital of Traditional Chinese Medicine, Kunming 650599, Yunnan, China. Tel: +86-18288941670; E-mail: 1271429684@qq.com (SJH); Tel: +86-13608819852; E-mail: kmglh169@163.com (LHG); Peng Chen, School of Pharmaceutical Sciences and Yunnan Key Laboratory of Pharmacology for Natural Products, Kunming Medical University, Kunming 650500, Yunnan, China. Tel: +86-13908713337; E-mail: ynkmcp@gmail.com; chenpeng@kmmu.edu.cn

References

[1] Paul S and Candelario-Jalil E. Emerging neuroprotective strategies for the treatment of ischemic stroke: an overview of clinical and preclinical studies. Exp Neurol 2021; 335: 113518.

[2] Feske SK. Ischemic stroke. Am J Med 2021; 134: 1457-1464.

[3] Jolugbo P and Ariëns RAS. Thrombus composition and efficacy of thrombolysis and thrombectomy in acute ischemic stroke. Stroke 2021; 52: 1131-1142.

[4] Kwok CS, Bains NK, Ford DE, Gomez CR, Hanley DF, Hassan AE, Nguyen TN, Siddiq F, Spiotta AM, Zaidi SF and Qureshi AI. Intra-arterial thrombolysis as adjunct to mechanical thrombectomy in acute ischemic stroke patients in the United States: a case control analysis. J Stroke Cerebrovasc Dis 2023; 32: 107093.

[5] Wassélius J, Arnberg F, von Euler M, Wester P and Ullberg T. Endovascular thrombectomy for acute ischemic stroke. J Intern Med 2022; 291: 303-316.

[6] Kapanova G, Tashenova G, Akhenbekova A, Tokpınar A and Yılmaz S. Cerebral ischemia reperfusion injury: from public health perspectives to mechanisms. Folia Neuropathol 2022; 60: 384-389.

[7] Mowla A, Razavi SM, Lail NS, Mohammadi P, Shirani P, Kavak KS, Sawyer RN and Kamal H. Hyperdense middle cerebral artery sign and response to combination of mechanical thrombectomy plus intravenous thrombolysis in acute stroke patients. J Neurol Sci 2021; 429: 117618.

[8] Si Z, Liu J, Hu K, Lin Y, Liu J and Wang A. Effects of thrombolysis within 6 hours on acute cerebral infarction in an improved rat embolic middle cerebral artery occlusion model for ischaemic stroke. J Cell Mol Med 2019; 23: 2468-2474.

[9] Chamorro Á, Dirnagl U, Urra X and Planas AM. Neuroprotection in acute stroke: targeting excitotoxicity, oxidative and nitrosative stress, and inflammation. Lancet Neurol 2016; 15: 869-881.

[10] Wang L, Liu C, Wang L and Tang B. Astragaloside IV mitigates cerebral ischaemia-reperfusion injury via inhibition of P62/Keap1/Nrf2 pathway-mediated ferroptosis. Eur J Pharmacol 2023; 944: 175516.

[11] Cheng CY, Kao ST and Lee YC. Angelica sinensis extract protects against ischemia-reperfusion injury in the hippocampus by activating p38 MAPK-mediated p90RSK/p-Bad and p90RSK/CREB/BDNF signaling after transient global cerebral ischemia in rats. J Ethnopharmacol 2020; 252: 112612.

[12] Gao L, Cao M, Li JQ, Qin XM and Fang J. Traditional Chinese medicine network pharmacology in cardiovascular precision medicine. Curr Pharm Des 2021; 27: 2925-2933.

[13] Wang L, Wu F, Hong Y, Shen L, Zhao L and Lin X. Research progress in the treatment of slow transit constipation by traditional Chinese medicine. J Ethnopharmacol 2022; 290: 115075.

[14] Lin J, Wang Q, Xu S, Zhou S, Zhong D, Tan M, Zhang X and Yao K. Banxia baizhu tianma decoction, a Chinese herbal formula, for hypertension: integrating meta-analysis and network pharmacology. Front Pharmacol 2022; 13: 1025104.

[15] Zhao L, Zhang H, Li N, Chen J, Xu H, Wang Y and Liang Q. Network pharmacology, a promising approach to reveal the pharmacology mechanism of Chinese medicine formula. J Ethnopharmacol 2023; 309: 116306.

[16] Li QF, Lu WT, Zhang Q, Zhao YD, Wu CY and Zhou HF. Proprietary medicines containing bupleurum chinense DC. (Chaihu) for depression: network meta-analysis and network pharmacology prediction. Front Pharmacol 2022; 13: 773537.

[17] Yang P, Tian YM, Deng WX, Cai X, Liu WH, Li L and Huang HY. Sijunzi decoction may decrease apoptosis via stabilization of the extracellular matrix following cerebral ischaemia-reperfusion in rats. Exp Ther Med 2019; 18: 2805-2812.

[18] Zhang Y, Yang M, Yuan Q, He Q, Ping H, Yang J, Zhang Y, Fu X and Liu J. Piperine ameliorates ischemic stroke-induced brain injury in rats by regulating the PI3K/AKT/mTOR pathway. J Ethnopharmacol 2022; 295: 115309.
[19] Bhati M, Thakre S and Anjankar A. Nissl granules, axonal regeneration, and regenerative therapeutics: a comprehensive review. Cureus 2023; 15: e47872.
[20] Guo R, Yi Z, Wang Y and Wang L. Network pharmacology and experimental validation to explore the potential mechanism of Sanjie Zhentong Capsule in endometriosis treatment. Front Endocrinol (Lausanne) 2023; 14: 1110995.
[21] Fan Z, Pu X, Li L, Li Q, Jiang T, Lu L, Tang J, Pan M, Zhang L and Chai Y. Mechanism of polygonum capitatum intervention in pulmonary fibrosis based on network pharmacology and molecular docking technology: a review. Medicine (Baltimore) 2023; 102: e34912.
[22] Yuan Y, Sheng P, Ma B, Xue B, Shen M, Zhang L, Li D, Hou J, Ren J, Liu J, Yan BC and Jiang Y. Elucidation of the mechanism of Yiqi Tongluo Granule against cerebral ischemia/reperfusion injury based on a combined strategy of network pharmacology, multi-omics and molecular biology. Phytomedicine 2023; 118: 154934.
[23] Luo S, Li H, Mo Z, Lei J, Zhu L, Huang Y, Fu R, Li C, Huang Y, Liu K, Chen W and Zhang L. Connectivity map identifies luteolin as a treatment option of ischemic stroke by inhibiting MMP9 and activation of the PI3K/Akt signaling pathway. Exp Mol Med 2019; 51: 1-11.
[24] Pandurangan AK and Esa NM. Luteolin, a bioflavonoid inhibits colorectal cancer through modulation of multiple signaling pathways: a review. Asian Pac J Cancer Prev 2014; 15: 5501-5508.
[25] Su J, Xu HT, Yu JJ, Yan MQ, Wang T, Wu YJ, Li B, Lu WJ, Wang C, Lei SS, Chen SM, Chen SH and Lv GY. Luteolin ameliorates lipopolysaccharide-induced microcirculatory disturbance through inhibiting leukocyte adhesion in rat mesenteric venules. BMC Complement Med Ther 2021; 21: 33.
[26] Zhang SS, Liu M, Liu DN, Shang YF, Du GH and Wang YH. Network pharmacology analysis and experimental validation of kaempferol in the treatment of ischemic stroke by inhibiting apoptosis and regulating neuroinflammation involving neutrophils. Int J Mol Sci 2022; 23: 12694.
[27] Yuan Y, Zhai Y, Chen J, Xu X and Wang H. Kaempferol ameliorates oxygen-glucose deprivation/reoxygenation-induced neuronal ferroptosis by activating Nrf2/SLC7A11/GPX4 axis. Biomolecules 2021; 11: 923.
[28] Zhang Y, Zhang H, Zhao F, Jiang Z, Cui Y, Ou M, Mei L and Wang Q. Mitochondrial-targeted and ROS-responsive nanocarrier via nose-to-brain pathway for ischemic stroke treatment. Acta Pharm Sin B 2023; 13: 5107-5120.
[29] Li G, Ye C, Zhu Y, Zhang T, Gu J, Pan J, Wang F, Wu F, Huang K, Xu K, Wu X and Shen J. Oxidative injury in ischemic stroke: a focus on NADPH oxidase 4. Oxid Med Cell Longev 2022; 2022: 1148874.
[30] Anilkumar N, San Jose G, Sawyer I, Santos CX, Sand C, Brewer AC, Warren D and Shah AM. A 28-kDa splice variant of NADPH oxidase-4 is nuclear-localized and involved in redox signaling in vascular cells. Arterioscler Thromb Vasc Biol 2013; 33: e104-e112.
[31] Moloney JN, Jayavelu AK, Stanicka J, Roche SL, O'Brien RL, Scholl S, Böhmer FD and Cotter TG. Nuclear membrane-localised NOX4D generates pro-survival ROS in FLT3-ITD-expressing AML. Oncotarget 2017; 8: 105440-105457.
[32] Yingze Y, Zhihong J, Tong J, Yina L, Zhi Z, Xu Z, Xiaoxing X and Lijuan G. NOX2-mediated reactive oxygen species are double-edged swords in focal cerebral ischemia in mice. J Neuroinflammation 2022; 19: 184.
[33] Pan N, Lu LY, Li M, Wang GH, Sun FY, Sun HS, Wen XJ, Cheng JD, Chen JW, Pang JY, Liu J, Guan YY, Zhao LY, Chen WL and Wang GL. Xyloketal B alleviates cerebral infarction and neurologic deficits in a mouse stroke model by suppressing the ROS/TLR4/NF-κB inflammatory signaling pathway. Acta Pharmacol Sin 2017; 38: 1236-1247.
[34] Huang J, Hu X, Li J and Gong D. Edaravone dexborneol promotes M2 microglia polarization against lipopolysaccharide-induced inflammation via suppressing TLR4/MyD88/NF-κB pathway. Naunyn Schmiedebergs Arch Pharmacol 2024; 397: 6647-6659.
[35] Dong X, Wang L, Song G, Cai X, Wang W, Chen J and Wang G. Physcion protects rats against cerebral ischemia-reperfusion injury via inhibition of TLR4/NF-kB signaling pathway. Drug Des Devel Ther 2021; 15: 277-287.
[36] Lietzau G, Sienkiewicz W, Karwacki Z, Dziewiątkowski J, Kaleczyc J and Kowiański P. The effect of simvastatin on the dynamics of NF-κB-regulated neurodegenerative and neuroprotective processes in the acute phase of ischemic stroke. Mol Neurobiol 2023; 60: 4935-4951.
[37] Man AWC, Li H and Xia N. Impact of lifestyles (diet and exercise) on vascular health: oxidative stress and endothelial function. Oxid Med Cell Longev 2020; 2020: 1496462.
[38] Zhao A, Sun Q, Zhang J, Hu T, Zhou X, Wang C, Liu J and Wang B. Substance basis and pharmacological mechanism of heat-clearing herbs

in the treatment of ischaemic encephalopathy: a systematic review and network pharmacology. Ann Med 2024; 56: 2308077.
[39] Yu Z, Su G, Zhang L, Liu G, Zhou Y, Fang S, Zhang Q, Wang T, Huang C, Huang Z and Li L. Icaritin inhibits neuroinflammation in a rat cerebral ischemia model by regulating microglial polarization through the GPER-ERK-NF-κB signaling pathway. Mol Med 2022; 28: 142.
[40] Ou Z, Zhao M, Xu Y, Wu Y, Qin L, Fang L, Xu H and Chen J. Huangqi Guizhi Wuwu decoction promotes M2 microglia polarization and synaptic plasticity via Sirt1/NF-κB/NLRP3 pathway in MCAO rats. Aging (Albany NY) 2023; 15: 10031-10056.
[41] Cassel SL and Sutterwala FS. Sterile inflammatory responses mediated by the NLRP3 inflammasome. Eur J Immunol 2010; 40: 607-611.
[42] Han PP, Han Y, Shen XY, Gao ZK and Bi X. NLRP3 inflammasome activation after ischemic stroke. Behav Brain Res 2023; 452: 114578.
[43] Sho T and Xu J. Role and mechanism of ROS scavengers in alleviating NLRP3-mediated inflammation. Biotechnol Appl Biochem 2019; 66: 4-13.